

# Elemental Distribution in Fossilized Dinosaur Bone

N. Zoeger<sup>1</sup>, A. R. Pyzalla<sup>2</sup>, F. Meirer<sup>1</sup>, C. Strel<sup>1</sup>, P. Wobrauschek<sup>1</sup>, S. Smolek<sup>1</sup>, A. Maderitsch<sup>1</sup> and G. Falkenberg<sup>3</sup>

<sup>1</sup>Vienna University of Technology, Atomic Institute, Stadionallee 2, 1020 Vienna, Austria

<sup>2</sup>Max-Planck-Institut für Eisenforschung GmbH, Max Planck Str. 1, 40237 Düsseldorf, Germany

<sup>3</sup>Hamburger Synchrotronstrahlungslabor HASYLAB am Deutschen Elektronen-Synchrotron, Notkestr. 85, 22603 Hamburg, Germany

Due to their extraordinary size sauropod dinosaurs are among the biologically most interesting vertebrates. Recent estimates based on photogrammetric measurements in actual skeletons or on scientific reconstructions place common sauropods consistently in the 15t to 50t category. Sauropods are tetrapods, a body similar to proboscideans (elephants) is combined with a very small head on a very long neck and a long tail. Due to the very long time that has passed since the sauropods lived (their diversity and range peak was in the Late Jurassic and they went extinct at the end of the Cretaceous, 65 million years ago) sauropod bones today are fossilized. During the burial and the fossilization of the sauropod bones, their organic parts degenerated and the bone histology, bone porosity, protein content, the crystallinity of the bone apatite, carbonate content, and their content of chemical species in general changed. Thus the determination of the elemental distribution in bones from dinosaurs can provide essential information when studying these diagenetic changes occurring during fossilization. Moreover the knowledge of the elements and their distribution in ancient fossil samples may allow for conclusions on the dietary habits of extinct animals.

Therefore we studied the elemental distribution in two dinosaur bones, one excavated from the Tendaguru beds, Tanzania and the other one from the sauropod beds of the Morrison formation in Utah, USA. All measurements have been carried out using the confocal  $\mu$ -XRF set up at beamline L [1]. For optimized excitation conditions the Ni/C multilayer was used and the primary photon energy was tuned to 18.5keV. In order to minimize self absorption effects in the sample surface near fluorescence scans have been performed. Since the resolution of the system has been determined to be  $17 \times 20 \times 15 \mu\text{m}^3$  (depth x lateral x height) for an incident photon energy of  $E=9.7 \text{ keV}$  step sizes for scanning were chosen to be  $10\mu\text{m}$  in each direction. The analytical difficulties for these samples comprehend the detection of fluorescence photons from chemical elements showing strong concentration variations over the inspected region of the sample. Therefore the Radiant-Vortex SDD available at beamline L, which should be able to process count rates up to 500000 counts per second was used throughout the whole experiments. Unfortunately, the detector electronics could not be properly implemented in the measurement system until the beginning of the experiment. Therefore different filters had to be used in order to avoid detector saturation. This circumstance lead to an extension of the measurement time per pixel in order to be able to detect the trace elements in the samples. Analysis time per pixel was typically set to 5s. Elemental maps were obtained using the micro-XRF software package (spectrum fitting performed by AXIL) installed at the beamline.

Results from a typical area scan are shown in figure 1. As already mentioned above the individual elements showed strong fluctuations in concentration and therefore in fluorescence intensities over the investigated area, which leads to problems in image formation. If a linear gray scale is used for displaying the element maps from minimum to maximum intensities, single points (or clusters) of high intensities (eg. at metal inclusions) lead to a degradation of the contrast for the rest of the image. This effect can be seen for example in the maps for Au, Cu, and Zn. To overcome this problem one could introduce a lower- and higher threshold for the intensities and use a linear scaling for the intensities in between the threshold levels. However, this procedure in the image forming process can not be accomplished without losing information in the element maps and requires heavy user input to the software for image generation. Therefore different image forming and image processing algorithms are being tested for this specific data sets at the moment, in order to get the most reliable information out of the measurements.

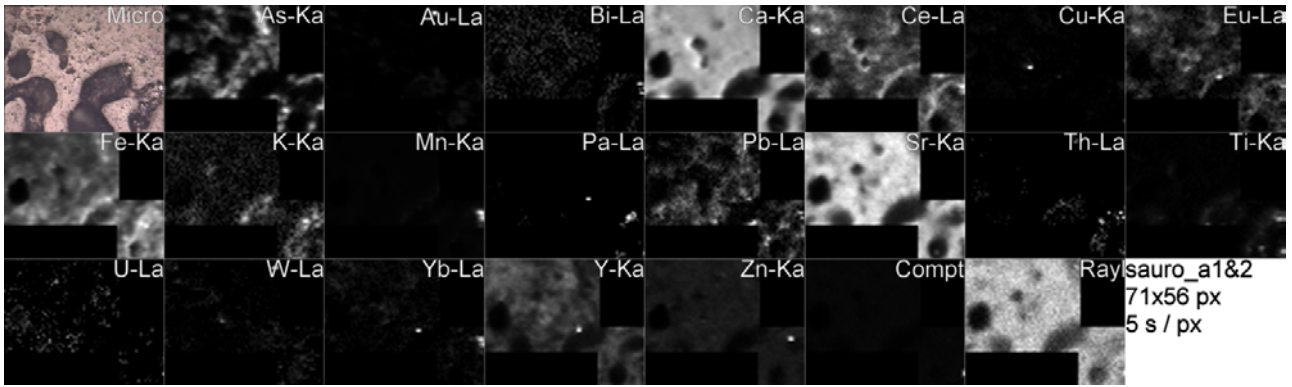


Figure 1: Optical micrograph (Micro) and elemental maps detected in a fossilized sauropod one from Utah, USA.

An additional problem occurred during the evaluation (AXIL-fitting) of the single spectra. In the AXIL fitting routine the theoretical ratios between the single X-ray lines within a line family are used for deconvolution of peak overlaps, which works reliable for standard (micro) XRF geometries. However, in the case of confocal (micro) XRF setups, the strong energy dependence of the detection volume and therefore the alteration in the ratios between e.g. the La and Lb line leads to a bad quality of the fit and to non-reliable results in the element maps. Whereas this circumstance does not play an important role for spectra with no peak overlaps it can not be neglected in this specific case where a large number of chemical elements are present in the sample and strong peak overlaps are observed (Figure 2).

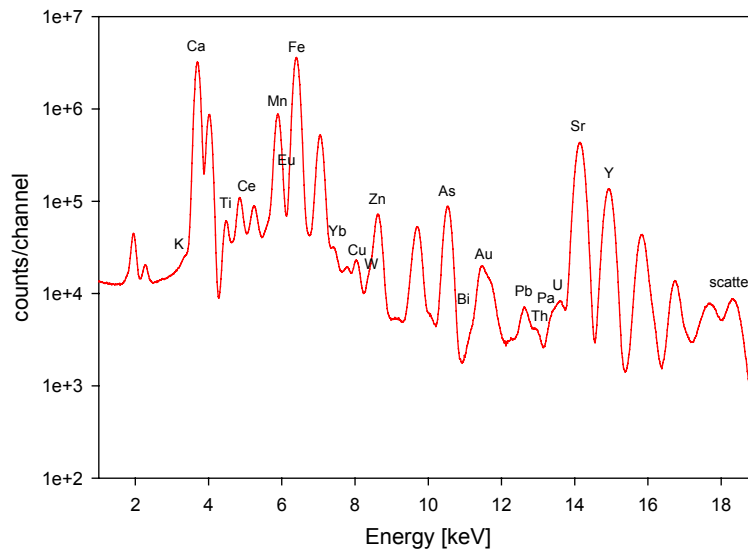


Figure 2: Sum spectrum over the entire scan region

Due to these mentioned difficulties, originating from the nature of the analyzed sample as well as from the measurement geometry special data treatment procedures are tested at the moment in order to obtain reliable results.

## References

- [1] K. Janssens, K. Proost, and G. Falkenberg, *Confocal microscopic X-ray fluorescence at the HASYLAB microfocuss beamline: characteristics and possibilities*. Spectrochimica Acta Part B: Atomic Spectroscopy, 2004. **59**(10-11): p. 1637-1645.